Supplementary Information

Ultra Small and Recyclable Zero-valent Iron Nanoclusters for Rapid and Highly Efficient Catalytic Reduction of P-nitrophenol in Water

Dongyang Shi,[a,b] Guifen Zhu,[a] Xiaodi Zhang,[a] Xia Zhang,[a] Xiang Li[a] and Jing Fan*[a]*

[a] School of Environment, Henan Key Laboratory for Environmental Pollution Control, Key Laboratory for Yellow River and Huai River Water Environment and Pollution Control, Ministry of Education, Henan Normal University, Xinxiang, Henan 453007, P. R. China.

[b] Henan Institute of Technology, Xinxiang, Henan 453003, P. R. China.

Corresponding Author

* E-mail: fanjing@htu.cn

1. Magnetic separation of the ZVI nanoclusters by a stronger magnet

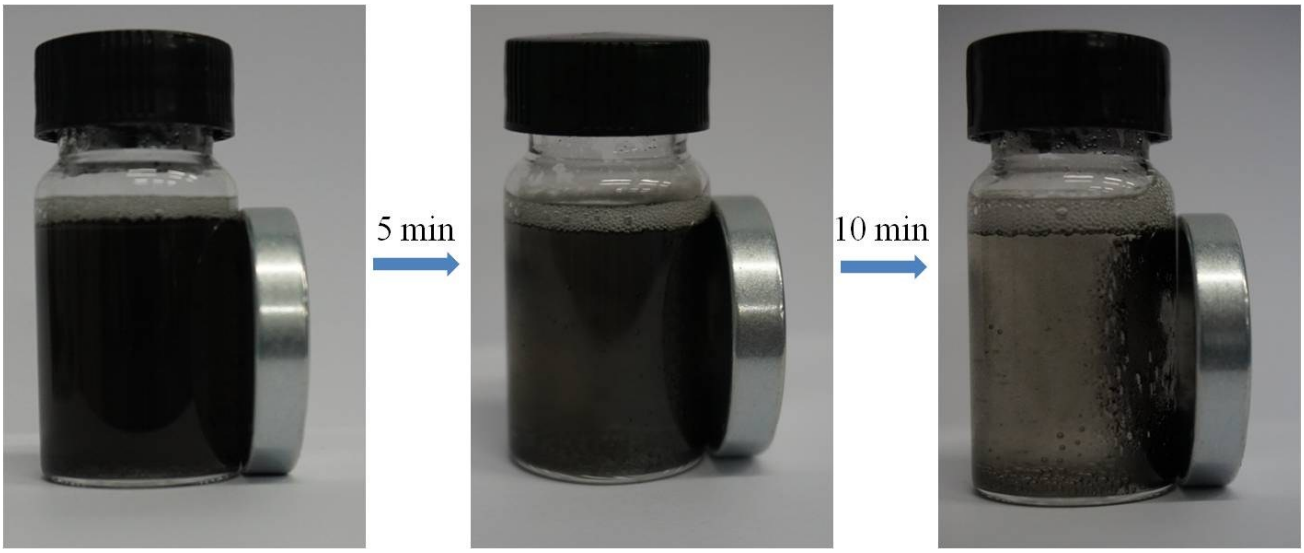

Fig. S1 Magnetic separation of the ZVI nanoclusters by a stronger magnet.

2. SEM image of ZVI nanoclusters and corresponding EDX elemental mapping images

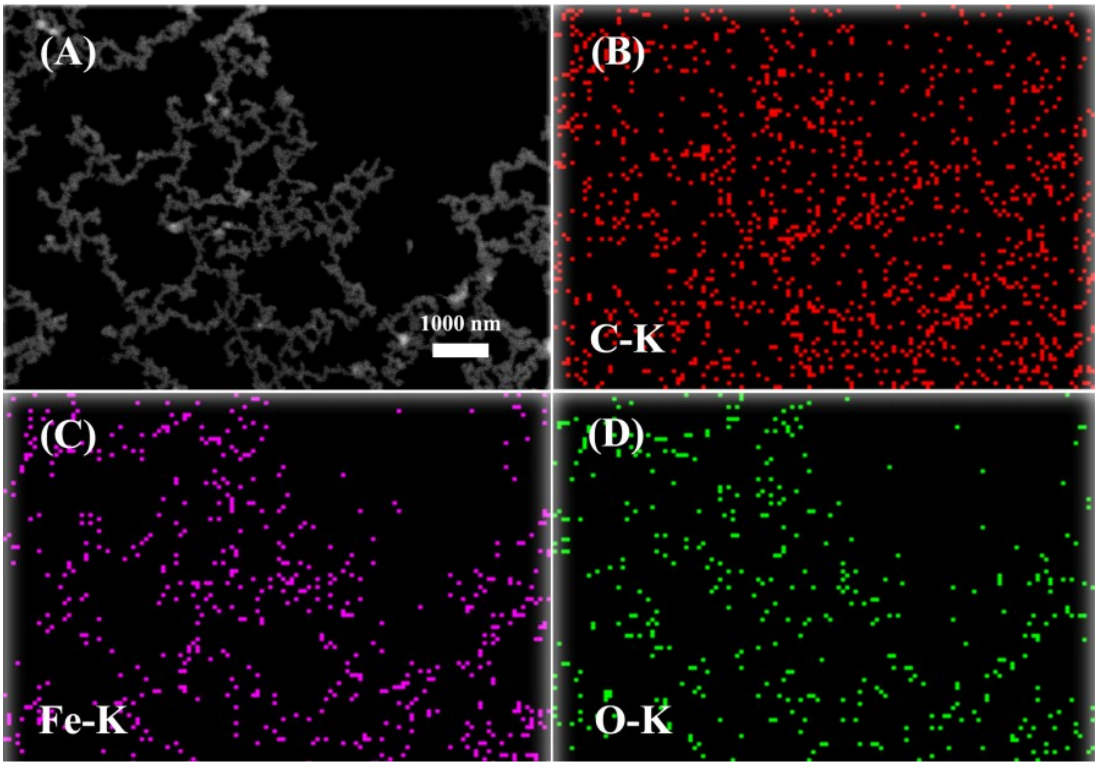

Fig. S2 SEM image of ZVI nanoclusters and corresponding EDX elemental mapping images.

3. Representative ^{57}Fe Mössbauer spectra of ZVI products

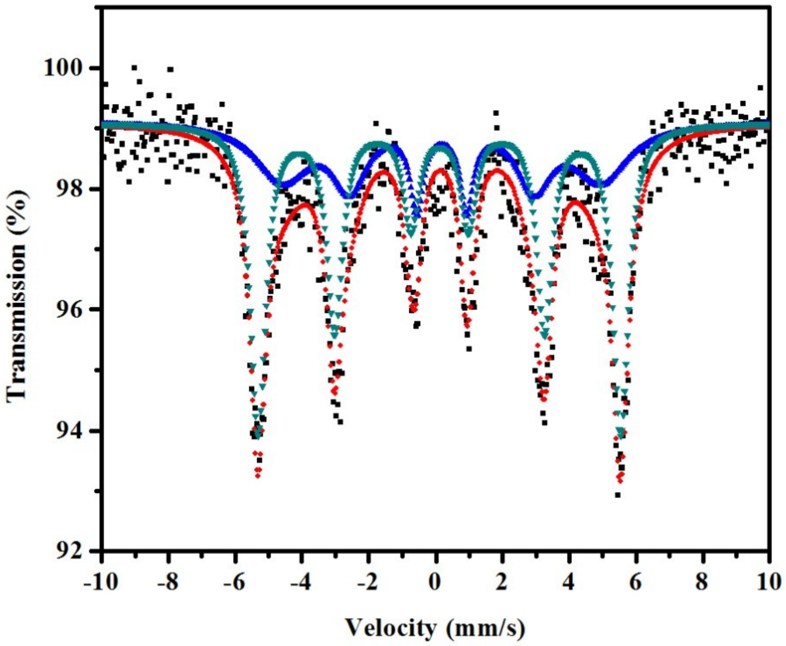

Fig. S3 Representative ^{57}Fe Mössbauer spectra of ZVI products. Mössbauer spectra were measured at 77 K. Key: green and blue, two sextets of α-Fe.

4. The size distribution histograms of the spherical CTAB micelles (A) and the assemblages of $CTA^+/FeBr_4^-$ complex

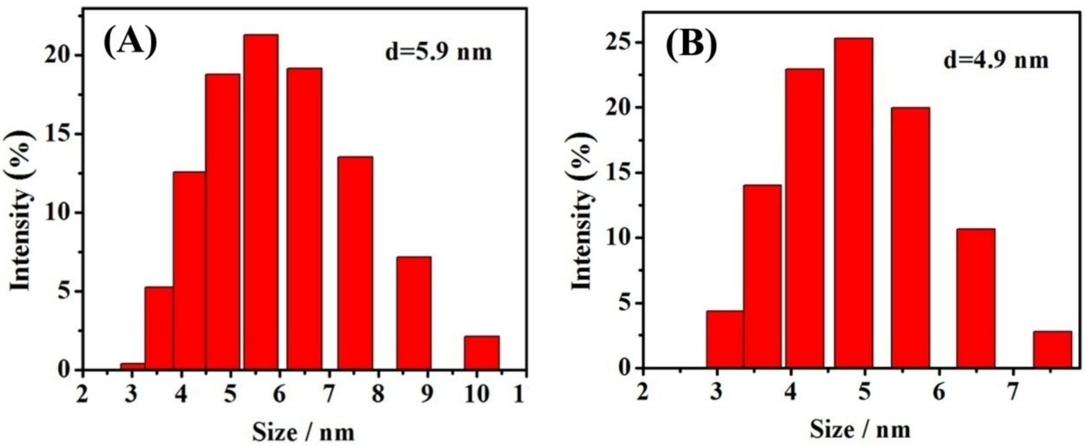

Fig. S4 DLS intensity-size distribution histogram of CTAB micelles (A) and $CTA^+/FeBr_4^-$ complex (B).

5. XRD patterns of FeS (intermediate product) and S

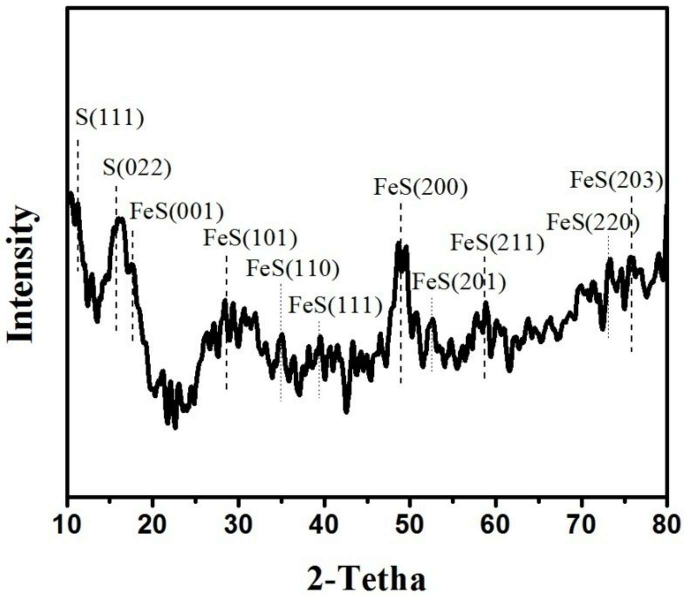

Fig. S5 XRD patterns of FeS (intermediate product) and sulphur.

6. High-resolution high-angle annular dark-field (HAADF) STEM image of sulfur nanoparicles and corresponding EDS elemental mapping images

ZVI nanoclusters suspension was sampled directly for STEM-EDS examination to evaluate the macroscopic composition of the nanoparicles. The signals of C-K, O-K, S-K and Fe-K as well as their distribution area were presented in Fig. S4, which confirmed that sulfur nanoparicles was one of representative end products in the reaction ($2Fe^{3+} + 3S^{2-} \rightarrow 2FeS + S$).

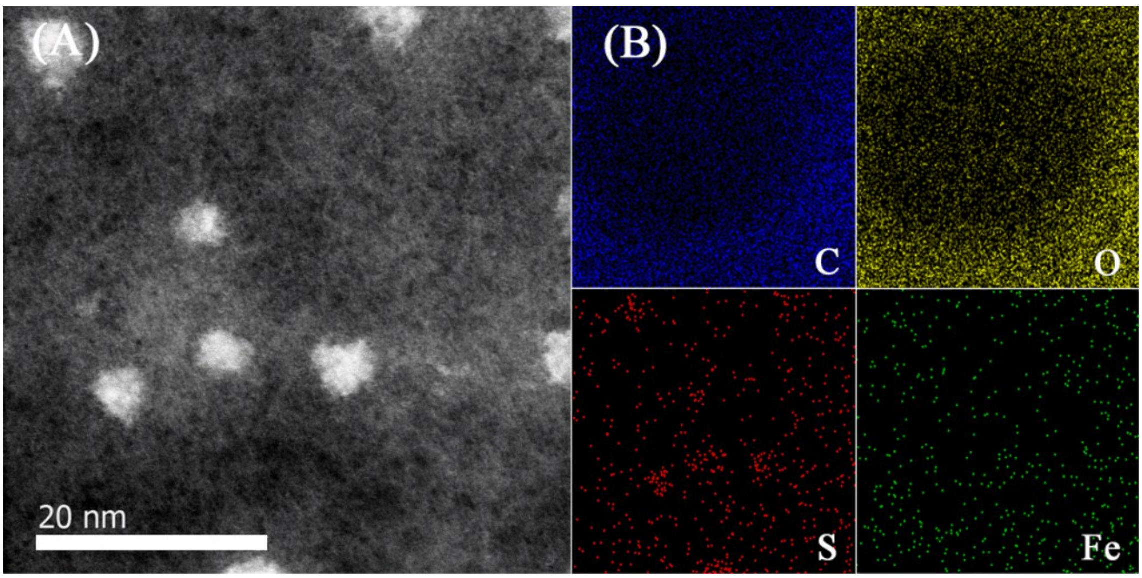

Fig. S6 High-resolution high-angle annular dark-field (HAADF) STEM image of sulfur nanoparicles (A) and corresponding EDS elemental mapping images (B).

7. Transmission electron microscope (TEM) image of the Fe^0 nanoparticles prepared without thiourea

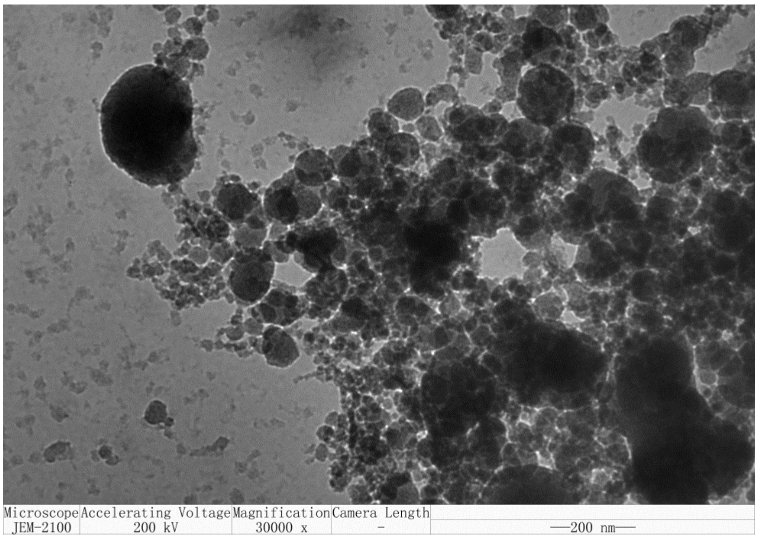

Fig. S7 TEM image of the Fe^0 nanoparticles prepared without thiourea.

8. The absorption of the filter membrane on p-nitrophenol

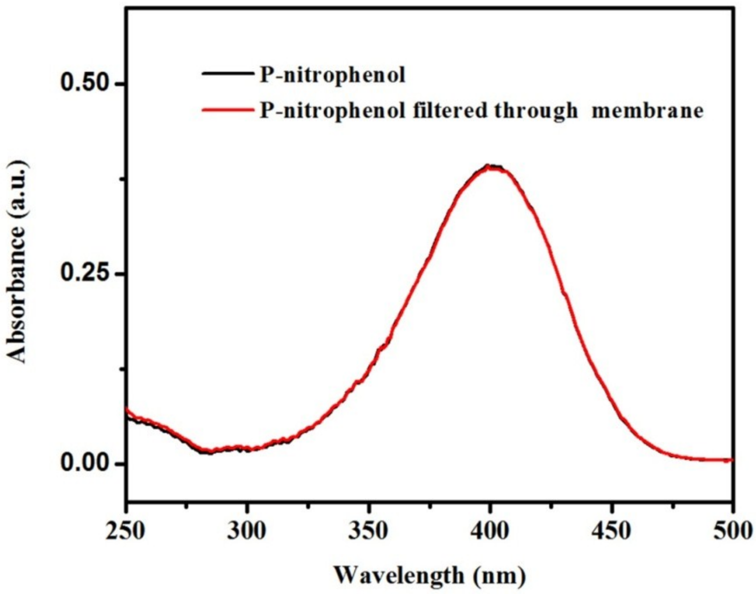

Fig. S8 The spectroscopic analysis of the p-nitrophenol aqueous solution before and after filtration through a 0.22 μm membrane.

9. Reduction of p-nitrophenol by ZVI nanoclusters and ZVI nanoparticles without $NaBH_4$

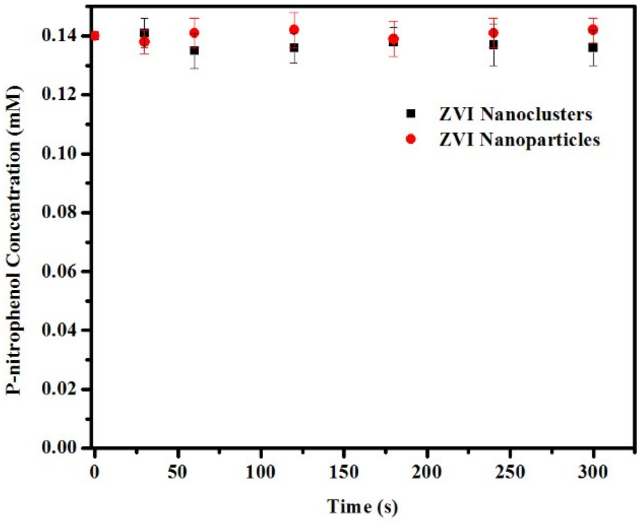

Fig. S9 Reduction of p-nitrophenol (0.14 mM) by ZVI nanoclusters (0.44 mM) and ZVI nanoparticles (0.44 mM) without $NaBH_4$ under inert condition. Reaction conditions: temperature, 20 °C; stirring speed, 180 rpm and reaction time, 300 s.

10. XPS analysis and XRD observation of the ZVI nanoclusters before and after reaction with p-nitrophenol in the absence of $NaBH_4$

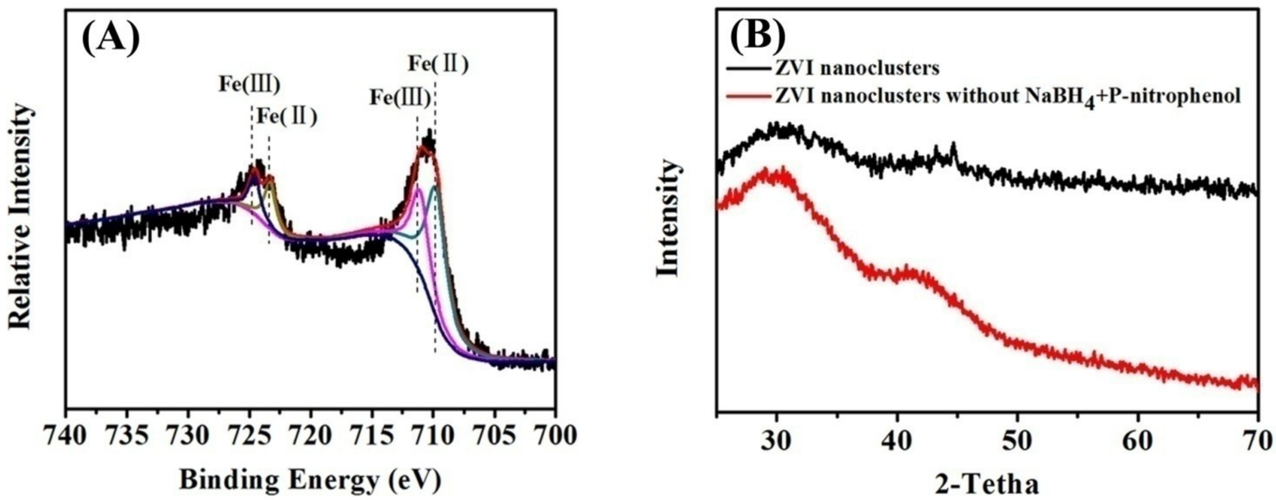

Fig. S10 XPS spectrum (A) for the narrow scan of Fe 2_P on the surface of ZVI nanoclusters after reaction with p-nitrophenol in the absence of $NaBH_4$, and XRD patterns (B) of ZVI nanoclusters before and after reaction with p-nitrophenol in the absence of $NaBH_4$.

11. HPLC of the samples after the p-nitrophenol degradation process

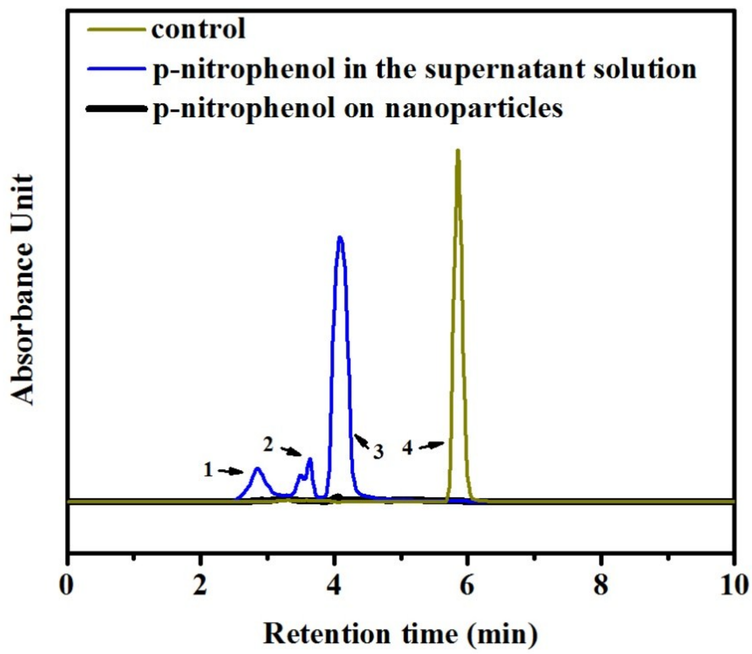

Fig. S11 HPLC of the samples in the reactor after the p-nitrophenol degradation process. 1, p-nitrosophenol; 2, p-hydroxylaminophenol; 3, p-aminophenol; 4, p-nitrophenol.

12. Global survey XPS spectra of nanoclusters before and after cycles

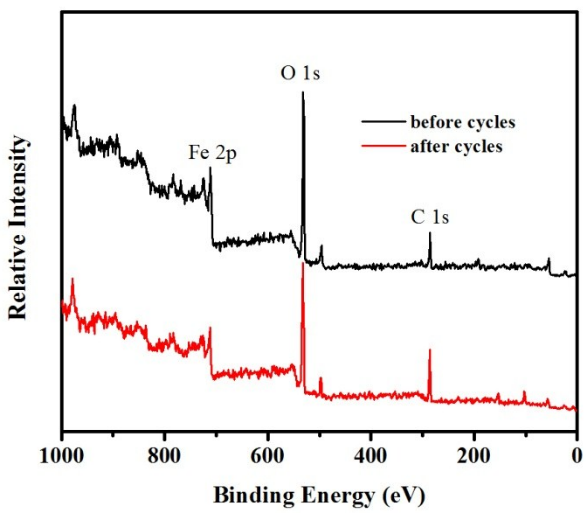

Fig. S12 Global survey XPS spectra of nanoclusters before and after cycles.

13. The mass percent content of Fe^0 in ZVI nanoclusters before and after eight reaction cycles and the TEM image of the ZVI nanoclusters after recycling tests

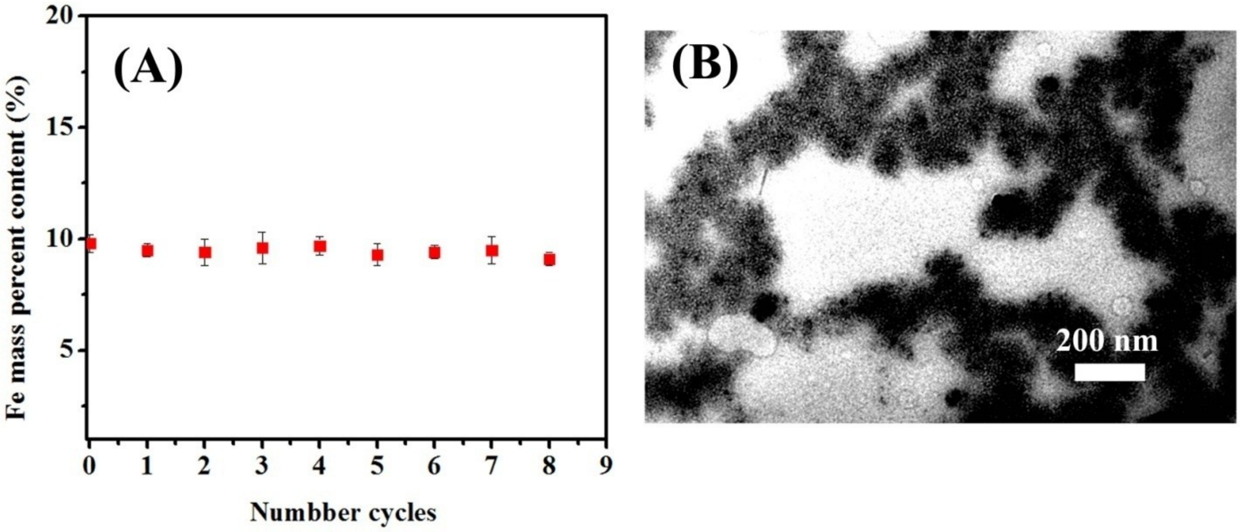

Fig. S13 The mass percent content of Fe^0 in ZVI nanoclusters (A) before and after eight reaction cycles, and TEM image of the ZVI nanoclusters (B) after eight recycling tests in the presence of $NaBH_4$.

14. Comparison for the reduction of p-nitrophenol with different catalysts

Table S1 Comparison for the reduction of p-nitrophenol with different catalysts at 20 °C

catalyst	$NaBH_4$: p-nitrophenol (mole ratio)	activity factor K_a(s^{-1} g^{-1})	conversion (100 %) time	reference
Au@C	100:1		5 min	1
Pd−CNT−GH	100:1		30 s	2
Ni/mesoporous carbons	1000:1	20.9	10 min	3
Pd	176:1	24.0	19.5min	4
Porous Cu microspheres	42:1	6	18 min	5
ZVI nanoparticles	433:1		30 min	6
Fe/CC-CH	167:1		28 min	7
Fe/fly ash	30000:1		60 min	8
Fe/ zeolite	1000:1	35.1	100 s	9
ZVI nanoclusters	100:1		<5 s	this work
ZVI nanoclusters	23:1	68.3	60 s	this work

References:

1 R. Liu, S. M. Mahurin and C. Li, *Angew. Chem. Int. Ed.*, 2011, **50**, 6799–6802.

2 Z. Zhang, T. Sun, C. Chen, F. Xiao, Z. Gong and S. Wang, *ACS Appl. Mater. Interfaces.*, 2014, **6**, 21035–21040.

3 Y. Yang, Y. Ren, C.-J. Sun and S.-H. Hao, *Green Chem.*, 2014,**16**, 2273–2280.

4 Y. Zhou and H.-C. Zeng, *J. Am. Chem. Soc.*, 2014,**136**, 13805–13817.

5 Y. Zhang, P.-L. Zhu, L. Chen, G. Li, F.-R. Zhou, D.-Q. Lu, R. Sun, F. Zhou and C.-P. Wong, *J. Mater. Chem. A.*, 2014, **2**, 11966–11973.

6 S. Bae, S. Gim, H. Kim and K. Hanna, *Appl. Catal. B: Environ.*, 2016, **182**, 541–549.

7. F. Ali, S. B. Khan, T. Kamal, K. A. Alamry, A. M. Asiri and T. R. A. Sobahi, *scientific reports*, 2017, **7**, 16957–16973.

8. J. Park and S. Bae, *Chemosphere*, 2018, **202**, 733–741.

9 A, Elfiad, D. C. Boffito, S, Khemassia, F, Galli, S. Chegrouche and L. Meddour-Boukhobza, *Can J Chem Eng*, 2018, **96**, 1566–1575.